Estimating the Effect of Carbon Emissions on Global Average Temperature

J. S. Reid[1], J. Dengler[2]

[1]33 Charlotte St., New Norfolk, Tas. 7140, Australia
[2]Reichensteinstr. 54, 69151 Neckargemünd, Germany

Key Points:

- Carbon emissions have increased CO2 concentration in the atmosphere and increased in global average temperature by 1 deg C.
- The quantity of remaining fossil fuel reserves suggest that further increases in global average temperature will be less than 1 deg C.
- The assumption that newly emitted carbon dioxide will remain in the atmosphere for millennia is not supported by observation.

Corresponding author: John Reid, `johnsinclairreid@gmail.com`

Abstract

The successful application of simple statistical methods in economic modelling suggest that similar methods could provide insight into global climate. We apply an autoregressive method to observed time series to determine the dependence of atmospheric CO_2 concentration on carbon emissions and, in turn, the dependence of globally averaged temperature on atmospheric CO_2 concentration. We ascribe physical meaning to the regression parameters in terms of first order differential equations describing the diffusion of CO_2 and heat between reservoirs, viz.: the diffusion of CO_2 between the atmosphere and the deep ocean and the transport of heat from the mixed layer. A strong feature of regression models is their built-in mechanism for deciding when a model provides an adequate description of the given data. Two implications of this statistically robust approach are that CO_2 diffuses from the atmosphere within a time scale of decades and that global average temperatures are unlikely to exceed $2°C$ above pre-industrial values.

Plain Language Summary

We use a conventional, statistical method to estimate the dependence of carbon concentration on emissions, and, in turn, to estimate the dependence of temperature on carbon concentration. Then, based on general assumptions about future emissions, we make realistic forecasts of global temperature and show that human caused CO_2 and its associated forcing are creating a temperature pulse and not a permanent plateau or self-amplifying feedback loop. There is no observational evidence that global climate is heading towards a catastrophe nor that carbon dioxide remains in the atmosphere indefinitely.

1 Introduction

In the early days of economic modelling it was found that complicated models performed poorly when used for out-of-sample forecasting. Regression models with few independent variables often produced better forecasts than did the big models (Nelson, 1972) (Ashley, 1988). Global Circulation Models are no less complicated than economic models but, until now, this aspect of them has been ignored. Furthermore, there are issues with the fundamental physics of GCMs because they are deterministic and do not allow for the Gibbs entropy associated with turbulence (Reid, 2019).

The fundamental question such models are designed to answer is the extent to which increases in atmospheric greenhouse gas concentrations affect the Earth's climate. We develop a simple physical model of the ocean-atmosphere system based on the diffusion of heat and carbon dioxide between reservoirs. This model has the advantage that regression methods can be used to estimate parameters from well-established time series data of emission, concentration and temperature. Once these parameters are known, they can be used to predict future CO_2 concentrations and global average temperature based on reasonable assumptions about future carbon emissions.

2 Diffusion and the ARX Model

By convention, a fluid is assumed to be a Newtonian continuum describable by differential equations such as the Navier-Stokes equations and diffusion equations. In practice, observations of fluids usually comprise time series, i.e. sequences of discrete numbers sampled or averaged over equal intervals of time. Time series can be related to continuous differential equations by means of finite difference approximations. Time series readily lend themselves to a statistical interpretation and allow high frequency noise and seasonal effects to be eliminated by choosing a suitable sampling interval.

The diffusion of a chemical constituent or heat between two reservoirs is described by Fick's Law. In one dimension

$$J = -D\frac{dc}{dz} \tag{1}$$

where J is the diffusion flux, D is the diffusion coefficient, c is the concentration and z is the spatial coordinate. Together with the continuity equation

$$\frac{\partial c}{\partial t} = F(t) - \oint J dA \tag{2}$$

this leads to the one dimensional diffusion equation

$$\frac{\partial c}{\partial t} + \oint \frac{D(c - c_0)}{\delta z} dA = F(t) \tag{3}$$

where $F(t)$ is the rate of pumping into the source reservoir, c_0 is the concentration in the sink reservoirs, δz is the thickness of the boundary layer between the two reservoirs and the integral is taken over the entire boundary layer area. (3) can be written

$$\frac{\partial c}{\partial t} + \frac{c}{\tau} = F(t) + \frac{c_0}{\tau} \tag{4}$$

where c is spatially homogeneous and τ is a constant which has the units of time. The second term on the right is generally negligibly small and can be subsumed into the forcing function, F, or ignored. In finite difference terms, with $c_0 = 0$, (4) becomes

$$\frac{c_i - c_{i-1}}{\Delta t} + \frac{c_i}{\tau} = F_i \tag{5}$$

69 where Δt is the time step or sampling interval, c_i and F_i designate values at time $i\Delta t$.

70 The above equations are deterministic and apply equally well to a numerical fluid
71 dynamical model as they do to the regression model we are developing here. However,
72 in order estimate model parameters from the data we need to develop a proper regres-
73 sion model and introduce random variables. We do this by making the forcing function,
74 $F(t)$, a random variable as the sum of a deterministic component, $f(t)$, and a random
75 component, ϵ_i, viz.:

$$F_i = f_i + \xi_i \tag{6}$$

76 where the expectation mean of ϵ_i is zero, i.e. $\mathbf{E}\xi_i = 0$ and $\mathbf{E}F_i = f_i$.

77 We now change notation so as to make a clear distinction between random vari-
78 ables (upper case) and constants (lower case). Equation (5) becomes

$$Y_i = \alpha_0 x_i + \alpha_1 y_{i-1} + \Xi_i \quad , \quad i = 1, ..., N \tag{7}$$

79 where $Y_i = c_i$, $x_i = f_i$, $y_{i-1} = c_{i-1}$,

$$\alpha_0 = \frac{\Delta t}{1 + \Delta t/\tau} \tag{8}$$

80 and

$$\alpha_1 = \frac{1}{1 + \Delta t/\tau} \tag{9}$$

81 This can be further generalized to

$$Y_i = \alpha_0 x_i + \sum_{j=1}^{p} \alpha_j . y_{i-j} + \sum_{k=1}^{q} \beta_j \Xi_{i-k} \quad , \quad i = 1, ..., N \tag{10}$$

82 where the atmospheric carbon concentration, c_i in (5), is represented by both Y and y,
83 $x_i = \Gamma_i$ is the exogenous variable and the Ξ_i are unselfcorrelated random variables with
84 zero mean. The regression coefficients α_0, α_j and β_j are to be estimated from the data
85 and p and q are small positive integers.

86 This is the ARMAX(p,q) model (for 'autoregressive moving average with exoge-
87 nous variable'). There are software packages for parameter estimation available under
88 the aegis of the major programming languages. Unfortunately some of these, such as the
89 Python *Statsmodels* package, are flawed, because they estimate the exogenous param-
90 eter, α_0, prior to estimating the other parameters, leading to omitted-variable bias (Greene,
91 2003).

92 Note the distinction between the random variable Y_i and the sample values y_{i-j}
93 which are constants. Equation (10) is a state space representation(Hamilton, 1994) de-
94 scribing states of the system at a succession of discrete instants; the random variable,
95 Y_i, at one instant becomes the constant, y_i, in the following instant. The direction of time
96 is important in regression, which, unlike correlation, allows causality to be inferred.

97 Estimation of the MA coefficients, $\{\beta_i\}$, requires an iterative Kalman filter method
98 which does not always converge. The second, moving average summation in (10) is a blur-
99 ring function, so that $q > 1$ when the sampling interval, Δt, is too small. The given
100 time series can be downsampled or 'decimated' by q to give a new time series with sam-
101 pling interval $q\Delta t$ with little loss of information and (10) becomes

$$Y_m = \alpha'_0 x_m + \sum_{n=1}^{p} \alpha'_n . y_{m-n} + \Xi'_m \quad , \quad m = 1, ..., M \tag{11}$$

where $m = qi$, $qM \leq N$ and

$$\Xi'_m = \sum_{k=1}^{q} \beta_j \Xi_{m-k} \tag{12}$$

so that $E(\Xi'_m \Xi'_n) = 0$ for $m \neq n$ because the summations do not overlap. The $\{\Xi'_m\}$ in (11) are therefore unselfcorrelated with zero mean. This is a simple case of a Renormalization Group Transformation(Wang et al., 2013). The aim here is to find the optimum scale for the given problem. In our case the optimum scale is considered to be the finest scale which satisfies the statistical test for the validity of the model.

The model summarized by (11) can be termed an ARX(p) model for 'autoregressive with exogenous variable'. Its parameters and their confidence limits can be estimated using ordinary least squares. The sequence of residuals, $\{\xi'_m\}$, is given by

$$\xi'_m = y_m - \left(\hat{\alpha}'_0 x_m + \sum_{n=1}^{p} \hat{\alpha}'_n . y_{m-n} \right) \quad , \quad m = 1, ..., M \tag{13}$$

where y_m is the sample value or 'realization' of Y_m, $\hat{\alpha}'_0$ and $\hat{\alpha}'_n$ are the coefficient estimates and the $\{\xi'_m\}$ are to be tested for self-correlation.

3 The Bomb Test Curve

Given the complexity of ocean-atmosphere interactions, the diffusion relationship (4) appears remarkably simple. However there is strong observational evidence that such a simple equation does indeed describe diffusion of atmospheric carbon into the ocean.

The testing of nuclear weapons during the 1950s and 1960s injected significant amounts of the radioactive ^{14}C isotope of carbon into the atmosphere. More importantly, the abrupt cessation of atmospheric testing following the Nuclear Test Ban Treaty of 5 August 1963, meant that the rate of production of the ^{14}C isotope reverted to the constant natural background level. This allows the movement of carbon dioxide between natural reservoirs to be assessed in much the same way that radioactive isotopes are used to assess metabolic processes in nuclear medicine.

The decrease in Δ^{14}C is known as "The Bomb Test Curve". Numerous observations were made in the decades following the cessation of testing following the Nuclear Test Ban Treaty. Here we look at a single high quality data set from Fruholmen, Norway (Nydal & Lövseth, 1983) shown in Figure 1. The natural logarithm, $\ln(\Delta^{14}C)$, is plotted on the vertical axis rather than Δ^{14}C itself so that exponential behaviour becomes linear. A regression line was fitted between January 1966 and the end of the data set in June 1993.

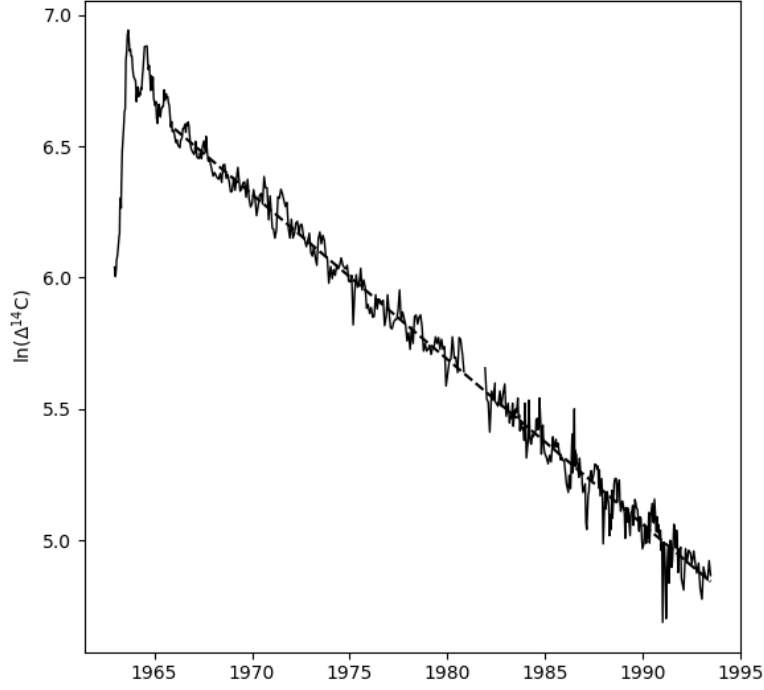| Statistic	Value
r	-0.9939
slope	-.06289 year^{-1}
τ	15.9 years
$t_{1/2}$	11.02 years

Table 1. Regression Statistics related to Figure 1

Figure 1. The natural logarithm of $\Delta^{14}C$ values recorded at Fruholmen, Norway as a function of time Dashed line: regression line fitted between January 1966 and June 1993.

.

Regression statistics are shown in Table 1. The fit is remarkably good and accounts for 98.8 percent of the variance. Hence, with a high degree of accuracy:

$$\Delta^{14}C = Ae^{-t/\tau} \tag{14}$$

where A is the value of $\Delta^{14}C$ at $t = 0$. Thus half of the bomb test $^{14}CO_2$ disappears from the atmosphere every 11 years[1].

Equation (14) is the solution of (4) with $c = \Delta^{14}CO_2$ and $F(t)$ specifies the rate at which concentration increases due to new material being introduced into the reservoir. There was a spike in $F(t)$ at the time of nuclear testing, after which it reverted to a constant background value due to the bombardment of upper atmosphere Nitrogen by cosmic rays.

Carbon dioxide reacts with water to form carbonate and bicarbonate ions. Hence the diffusion rate of carbon *per se* involves reaction rates and diffusion rates for each of these three species. These are almost completely independent of atomic mass(Zeebe, 2011) and so all the isotopes of carbon, ^{12}C, ^{13}C, ^{14}C, in the form of CO_2 and its radicles, dif-

---

[1] Note that this half-life of atmospheric $^{14}CO_2$ is due to diffusion of this gas from the atmosphere and is unrelated to the radioactive half-life of ^{14}C of 5730 years

142 fuse through water at the same rate and the time constant, τ, applies equally to all iso-
143 topic species of CO_2.

144 It is therefore reasonable to assume that CO_2 diffuses from the atmosphere into
145 some other reservoir or sink. The excellent fit of a single regression line indicates that
146 any diffusion process must be dominated by a single sink with a single time constant and
147 that this sink is not approaching saturation. Furthermore the fact that the atmospheric
148 $\Delta^{14}CO_2$ has, by now, returned to its pre-bomb background level implies that the sink
149 is much larger than the source, the atmosphere. The only candidate sink which fulfils
150 these conditions is the deep ocean.

4 Heat Transport

152 Environmental temperatures are laregly dependent on the transport of heat and
153 other forms of energy by turbulent processes(Hasselmann, 1976). Heat diffuses in the same
154 way as chemical constituents described by (1) and (2) leading to Fourier's heat equation:

$$\rho_0 c_p \frac{\partial T}{\partial t} = -\oint_A K_0 \frac{\partial T}{\partial z} dA + Q(x,t) \tag{15}$$

155 where ρ_0 and c_p are the density and specific heat of a reservoir, T is its temperature, t
156 is the time, z is a spatial variable with the units of length, K_0 is the conductivity or sim-
157 ilar constant, Q is the flux of heat or other form of energy and A is the surface area of
158 the reservoir.

159 In the present case the reservoir is the mixed layer of the ocean. Because the spe-
160 cific heat of water is much larger than that of air, the top 2.5 m of the mixed layer holds
161 as much heat as the entire atmosphere above it. The globally averaged mixed layer depth(de
162 Boyer Montgut et al., 2004) is about 100m, so that the heat capacity of the mixed layer
163 is 40 times that of the atmosphere. Seventy percent of the Earth's surface is ocean. Ef-
164 fectively, mixed layer temperatures comprise the bulk of globally averaged surface air tem-
165 perature measurements and the two measurements are highly correlated.

166 Integrating (15) over the entire mixed layer and including a radiative forcing term,
167 $G(t)$, for the heat trapping effect of greenhouse gases gives Newton's Law of Cooling for
168 the mixed layer:

$$\rho c_p \frac{\partial T}{\partial t} = -KT + G(t) + q(t) \tag{16}$$

169 where ρ, c_p are the density and specific heat of sea water and K is a global average of
170 all forms of cooling which are approximately proportional to temperature differences, i.e.
171 conduction via the thermocline into the deep ocean and convection to the top of the at-
172 mosphere to be radiated into space. $q(t)$ is the random component of heat gained and
173 lost by the mixed layer due to clouds and similar unpredictable phenomena.

174 In finite difference form (16) becomes

$$T_i = a.T_{i-1} + b.\Gamma_i + \xi_i \ , \ \ i = 1, ..., N \tag{17}$$

175 where $t = i\Delta t$, $\xi_i = \Delta t q_i/(\rho c_p + K\Delta t)$ and a and b are constants to be estimated from
176 the N data values. Γ_i is given by

$$\Gamma = \ln([CO_2]) \tag{18}$$

177 where $[CO_2]$ is the atmospheric carbon dioxide concentration in parts per million (Huang
178 & Shahabadi, 2014). This too can be further generalized to the form (10).

Model	Exogenous Variables	Q	P
ARX(0)	E_i only	1424.6	0.0000
ARX(1)	E_i,C_{i-1}	95.4	0.0000
ARX(2)	E_i,C_{i-1},C_{i-2}	120.0	0.0000
ARX(3)	E_i,C_{i-1}, ... ,C_{i-3}	91.3	0.0000
ARX(4)	E_i,C_{i-1}, ... ,C_{i-4}	71.0	0.0000
ARX(5)	E_i,C_{i-1}, ... ,C_{i-5}	71.4	0.0000

Table 2. Ljung-Box parameter, Q, and its probability, P, for ARX models of undecimated CO_2 concentration, C_i, and CO_2 emissions data, E_i.

5 Finding Models

We investigated the relationships between the the three time series: anthropogenic emissions, atmospheric CO_2 concentration and global average temperature. We did so by estimating the coefficients α'_0 and α'_n in the ARX model, (11), using Ordinary Least Squares. All coefficients were estimated simultaneously to avoid omitted-variable bias and the complexities of de-convoluting a moving average component were avoided by decimating the data when necessary.

We used the model twice; to estimate firstly, (i) the regression of atmospheric carbon concentration, C, on anthropogenic carbon emissions, E, and then, (ii) the regression of global average temperature anomaly, T, on the logarithm of atmospheric carbon concentration, Γ, estimated from step (i). In step (i), E is the exogenous variable. In step (ii) Γ is the exogenous variable.

In each case we used the model with $q = 0, 1, ..., 5$ ($q = 0$ implying that the second term on the RHS of (11) is omitted) in order to determine the smallest value of q for which the residuals given by (13) could be deemed unselfcorrelated. The successful models were then used to forecast global average temperature from Hubbert curves of emission estimates (Hubbert, 1962).

The *sine qua non* of all regression models is that the innovation, Ξ, be unselfcorrelated. It is an assumption which can be validated by testing whether the sample residuals, $\{\xi'_m\}$, given by (13), are self-correlated. If they are, then the random variables, $\{\Xi'_m\}$, in (11) cannot be assumed to be unselfcorrelated and (11) is not a valid regression model.

The Ljung-Box test parameter, Q, is computed from the sample autocorrelation of $\{\xi'_m\}$ at lag k out to some maximum lag, k_{max} (Ljung & Box, 1978). Under the null hypothesis that the residuals are unselfcorrelated, Q has a χ^2 distribution with $k - n$ degrees of freedom where n is the number of regression coefficients fitted. From this a probability, P, can be found and suitable values of q, the decimation factor, and p, the number of autoregressive coefficients. By Occam's Razor we chose the smallest values which satisfy this test.

Step (i): applying Ljung-Box to the residuals given by (13) for ARX(p), p= 0, ... ,5) gives the results shown in Table 2. Probabilities are zero for all values of p indicating that the null hypothesis that the residuals are unselfcorrelated can be rejected. Both time series were then decimated by 2. The results are shown in Table 3. The probability, P, for the ARX(1) model has a value of 0.4259 indicating that the null hypothesis that the residuals are unselfcorrelated cannot be rejected. The ARX(1) case, is a good fit to the decimated data and constitutes a valid regression model for C on E.

Step (ii): an ARX model of the regression of global average temperature, T, on the logarithm of atmospheric CO_2 concentration is also required. These time series were also

Model	Exogenous Variables	Q	P
ARX(0)	E_i only	513.5	0.0000
ARX(1)	E_i,C_{i-1}	28.5	0.4359
ARX(2)	E_i,C_{i-1},C_{i-2}	28.6	0.3830
ARX(3)	$E_i,C_{i-1}, ... ,C_{i-3}$	24.5	0.5483
ARX(4)	$E_i,C_{i-1}, ... ,C_{i-4}$	24.3	0.5049
ARX(5)	$E_i,C_{i-1}, ... ,C_{i-5}$	22.0	0.5796

Table 3. Ljung-Box parameter, Q, and its probability, P, for ARX models of CO_2 concentration, C_i and CO_2 emissions, E_i, when both time series have been decimated by 2

Model	Exogenous Variables	Q	P
ARX(0)	T_i vs $\ln(C_i)$ only	158.4	0.000
ARX(1)	T_i vs $\ln(C_i),T_{i-1}$	60.9	0.0003
ARX(2)	T_i vs $\ln(C_i),T_{i-1},T_{i-2}$	32.9	0.1995
ARX(3)	T_i vs $\ln(C_i),T_{i-1}, ... ,T_{i-3}$	31.2	0.2214
ARX(4)	$T_i)$vs $\ln(C_i),T_{i-1}, ... ,T_{i-4}$	32.5	0.1436
ARX(5)	T_i vs $\ln(C_i),T_{i-1}, ... ,T_{i-5}$	34.2	0.0807

Table 4. Ljung-Box parameter, Q, and its probability, P, for ARX models of global average temperature and CO_2 concentration data decimated by 2

Model	$\hat{\alpha}'_0$	$\hat{\alpha}'_1$	$\hat{\alpha}'_2$
C_i vs E_i, C_{i-1}	0.210	0.969	
T_i vs $\ln(C_i),T_{i-1},T_{i-2}$	1.549	0.213	0.299

Table 5. Regression coefficients estimated from the selected models

decimated by 2 to keep the same sampling interval throughout. The results of the Ljung-Box test for these ARX models are shown in Table 4. The ARX(2) model was chosen as the simplest model with unselfcorrelated residuals. Estimates of the regression coefficients of (11), $\hat{\alpha}'_0$, $\hat{\alpha}'_1$ and $\hat{\alpha}'_1$ for the two selected models are shown in Table 5

The ARX(1) model of Step (i) could equally well have been derived by simply estimating the regression of the first difference of observed CO_2 concentration on CO_2 emissions. However the present formalism led to recognition of the need to decimate these time series by two in order to satisfy the Ljung-Box test.

6 The Impulse Response Function of CO2 Concentration

The impulse response of a system is its output in response to a brief input signal. It completely characterises a linear time-invariant system; once the impulse response is known, the output corresponding to any input can be found by convolution. For continuous time systems the impulse response is related to the characteristic equation of the differential equations describing the system. In discrete time systems the impulse response can by found experimentally by applying appropriate regression methods to the measured input and output time series.

In assessing the effect of various greenhouse gases on global climate, the impulse responses of climate parameters such as global average temperature to various greenhouse gas inputs are of major importance. This has been done for a number of gases in order to determine their "Global Warming Potential", for example by Joos et al. (2013). Various computed impulse response functions of the atmospheric concentration of CO_2 in response to global emissions are shown in their Figure 1a. In every case more than 20 percent of the emitted pulse supposedly remains in the atmosphere after 1000 years. Sim-

ilar results have been used by modellers as far back as the First IPCC Assessment Report as shown in their Figure 8.

Although presented as such, the long-duration impulse responses for atmospheric CO_2 described by Joos et al are not derived from observations of the real world. They are not based on observation; they are all derived from global circulation models. The use of a fluid dynamical model as a surrogate for the real world only works if the model is homologous with the real world, i.e. there must be an *exact* correspondence in *every* aspect of the model; the correspondence between a handful of model averages and their real world values is not sufficient. In the present case the long-duration of the model-derived, CO_2 impulse response is most likely due to there being too little interaction between the atmosphere and the deep ocean in the GCMs. The sequestration of CO_2 in this very large, deep-ocean reservoir would be greatly inhibited in such a model.

The duration of the CO_2 impulse response is crucial in forecasting future climate and in planning emission reductions. It is important that it be estimated from real world observations.

It is clear from Figure 1 and Table 1 that the impulse response of atmospheric $\Delta^{14}C$ is exponential with a half time in the atmosphere of 11 years. The presence of bomb test $\Delta^{14}C$ can no longer be detected because it has fallen below the level of the $\Delta^{14}C$ created naturally by cosmic rays. There is no remaining twenty percent left over to last for a thousand years.

It might be argued that Bomb Test Curve is not a fair test of the Joos et al impulse response because it only shows the carbon being absorbed. There are only very small pre-existing $\Delta^{14}C$ values in the deep ocean, whereas there are regions of the ocean where CO_2 exceeds atmospheric values and diffusion will occur in the opposite direction. In the first case the integrand, $D(c-c_0)/\delta z$, in (3) is always positive whereas in the second case the integrand can be either positive or negative leading to a different net diffusion rate and a different time constant.

The impulse response function of atmospheric CO_2 concentration is the characteristic equation of (4) which is exponential. The time constant, τ, is found by substituting α_1 from Table 5 (0.969) into (9) which gives $\tau = 62.5$ years, once again, much less than the millennial time scales postulated by Joos et al. The difference between the half life time from the bomb tests of 11 years and the time constant from the regression is explained by the obvious fact, that the bomb test curve only measures absorption of CO_2 in the ocean, whereas our regression also measures the delaying effect of outgassing CO_2 from the ocean to the atmosphere.

7 Forecasting Global Average Temperature

Numerical fluid dynamical models such as GCMs are not well suited to prediction because they are fundamentally unstable and must often be damped by setting artificially high values of model parameters such as viscosity. Their value lies in providing insight into underlying physical processes. On the other hand, regression models are well suited to prediction when future values of exogenous variables are known or can be estimated. Their statistical nature allows hypothesis testing and the provision of confidence limits whereas GCMs require computationally expensive and statistically dubious "ensembles" of model runs for this purpose.

Using regression models for prediction purposes is based on a single assumption which may or may not be warranted depending on the circumstances: it is the assumption of covariance stationarity. Under this assumption regression coefficients estimated from the data, such as those of Table 5, can be substituted back into (11) to yield expectation values of Y outside the domain of the original data over the domain in which
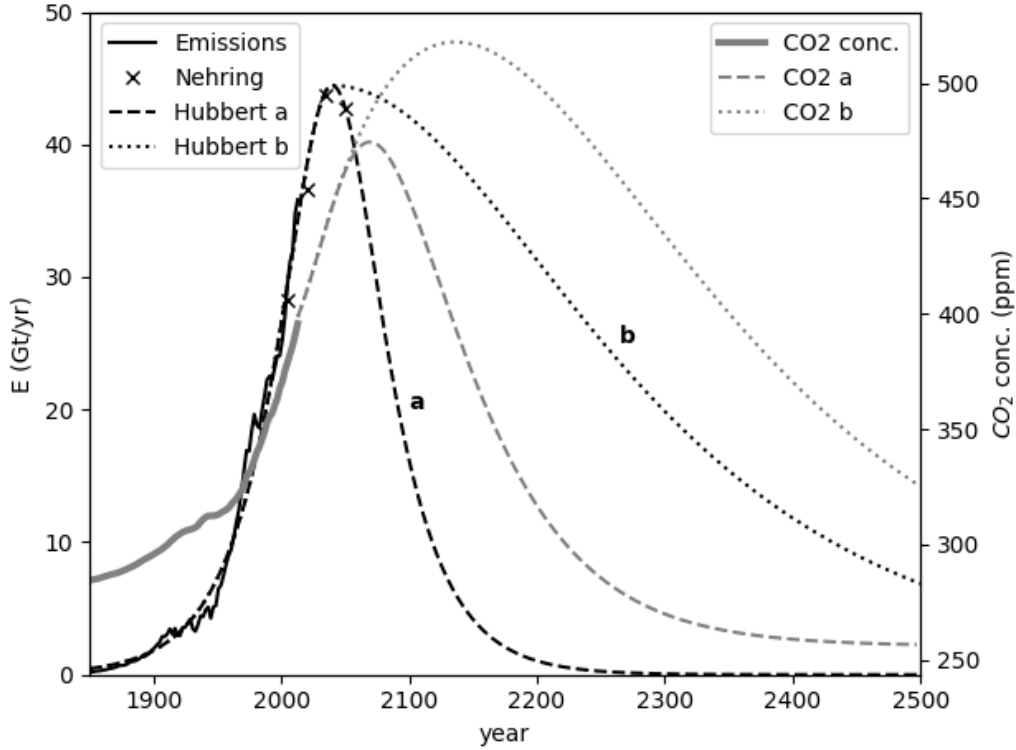
Figure 2. The solid black curve shows the recorded total carbon dioxide emission rate (Gt/yr). The crosses show recorded and predicted emission rates quoted by Nehring(Nehring, 2009). Curve **a** is the symmetrical Hubbert curve which best fits Nehring's data. Curve **b** is an asymmetrical Hubbert curve with decay time constant set to five times the onset constant. The grey dashed and dotted curves show the predicted CO_2 concentrations forecast from the two Hubbert emission curves.
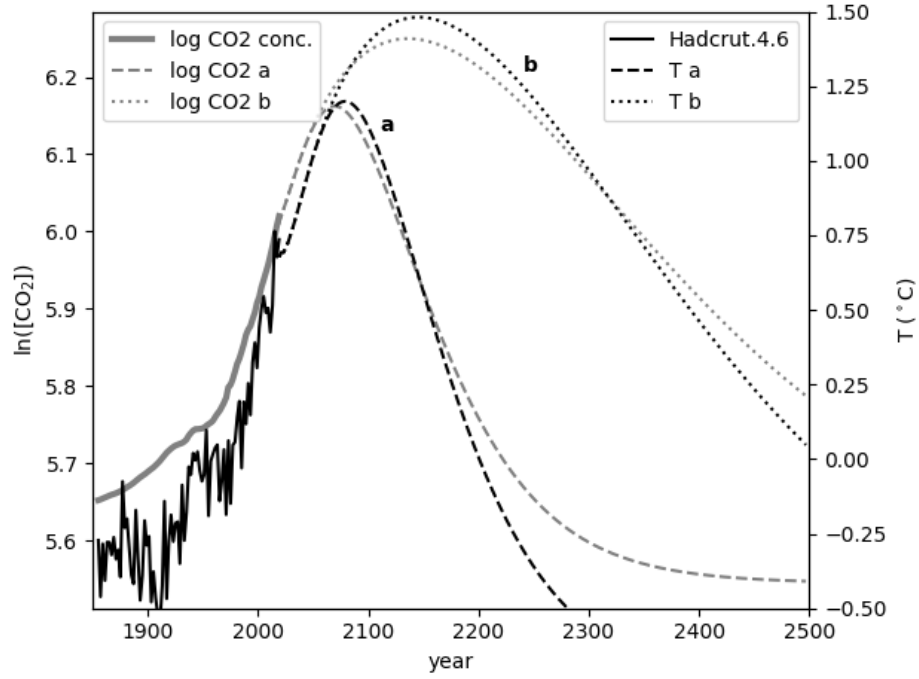
Figure 3. The grey curves show the logarithm of carbon concentrations resulting from the emission curves shown in Figure 2. The solid black curve is the observed (HadCRUT.4.6.0.0) global average temperature anomaly. The dashed black curves show the predicted global average temperature anomalies corresponding to the Hubbert curves **a** and **b** in Figure 2.

the exogenous variable, x, is known or can be estimated. This can be done by iteration. Thus, from (11)

$$\mathrm{E}(Y_{M+1}) = \alpha'_0 x_M + \sum_{n=1}^{p} \alpha'_n . y_{M+1-n} \tag{19}$$

since $\mathrm{E}(\Xi'_m) = 0$ by definition. If y_{M+1} is now defined as $\mathrm{E}(Y_{M+1})$ for substitution into the right hand side of (19), the process can be repeated and the future behaviour of the endogenous variable, y, forecast over the domain for which the exogenous variable, x, is known.

In order to forecast global average temperature we need to know the endogenous variable, Γ, a function of atmospheric carbon dioxide concentration, C, given by (18). In order to forecast C we need to know the carbon dioxide emission rate, E.

Although controversial, the Hubbert curve(Hubbert, 1962) provides a canonical starting point. The Hubbert curve for projected carbon emissions, fitted to known emissions and to the data of Nehring (Nehring, 2009) is shown as the dashed black curve, **a**, of Figure 2. The atmospheric CO_2 concentration forecast using the iterative method is shown as the grey dashed line.

A major criticism of the Hubbert Curve is its symmetry. In reality, the decline in resources is usually significantly slower than the onset of the curve. The dotted black curve, **b**, in Figure 2, shows an asymmetrical Hubbert curve with the same onset and maximum as curve **a**, but with a decay time which is five times slower. The corresponding, atmospheric CO_2 forecast is shown as the grey dotted line.

The emissions-generated, grey CO_2 concentration curves in Figure 2 were used via (18) to generate the (grey) log concentration curves **a** and **b** shown in Figure 3.

8 Data Sources

Time series in the form of annual averages of the relevant variables, E, C and T were downloaded from the Web in November 2020.

The global average temperature anomaly data, T. were taken from the `HadCRUT` `.4.5.0.0` data set(Morice et al., 2012).

Carbon dioxide concentrations, C, were taken from the University of Melbourne Greenhouse Gas Factsheet(Mainshausen et al., 2017) supplemented with recent values from Mauna Loa.

Global fossil fuel emissions, E, were downloaded from CDIAC, the Carbon Dioxide Information Analysis Center(Boden et al., 2017).

9 Results

The temperature anomaly forecasts generated from the two Hubbert scenarios are shown as the black dashed and dotted curves labelled **a** and **b** in Figure 3. The dashed curve, **a**, predicted from the symmetrical Hubbert curve has a maximum in the year 2079 with an anomaly value of $1.20°C$ (i.e. $1.57°C$ above the value in 1850 and $0.46°C$ above the value in 2020). The dotted curve, **b**, predicted from the asymmetrical Hubbert curve has a maximum in the year 2145 with an anomaly value of $1.48°C$ (i.e. $1.85°C$ above the value in 1850 and $0.74°C$ above the value in 2020).

The total emissions for the two Hubbert curves for the 650 years displayed in Figure 2 are also of interest, viz.: **a** 1824 Gt CO_2 and **b** 6223 Gt CO_2. Thus the total emissions for the Hubbert (b) curve are more than three times those for the Hubbert (a) curve

but the resulting temperature maxima differ by only 0.28°C. It follows that peak global average temperature is only a weakly dependent on total carbon emissions.

10 Conclusions

This work began as an attempt to estimate Climate Sensitivity using rigorous regression methods. Climate Sensitivity is defined as the temperature response to a sustained doubling of atmospheric CO_2 concentration and is used for the inter-comparison of GCMs. We soon realized that the concept itself is unrealistic because, according to (4) , CO_2 diffuses into the ocean at a rate proportional to its concentration so that, in order to sustain the higher concentration, a high rate of emissions would need to be sustained indefinitely. Given the finite nature of viable hydrocarbon resources, this is an unrealistic scenario.

Viewed on a time scale of centuries, human exploitation of fossil fuels in the industrial era is generating a pulse in atmospheric carbon concentration termed "Peak Carbon". This, in turn, generates a pulse in global average temperature. The world is presently in the onset phase of this pulse; reasonable estimates of recoverable fossil fuel reserves suggest that the Peak Carbon pulse will reach a maximum within the next century or so. Global average temperature will follow suit with a maximum value which is less than 2°C above pre-industrial values.

The impulse response of atmospheric CO_2 concentration is the response caused by a hypothetical, short variation in CO_2 emissions. The supposed, long-lived impulse response, widely accepted by the climate modelling community, is the most egregious flaw in the application of numerical global circulation models to climate. It implies that CO_2 emitted now will linger in the atmosphere for millennia. It sets the scene for the various catastrophes and tipping points presented in IPCC reports and justifies stringent emission regulations. It is based on the unwarranted assumption that GCMs provide a precise description of the ocean/atmosphere system as if it were some sort of clockwork mechanism. In contrast, our statistical model implies that the atmospheric concentration of CO_2 is self-regulated by diffusion into the deep ocean and that the small perturbation of the global environment caused by the combustion of fossil fuels will be brief.

References

Ashley, R. (1988). On the relative worth of recent macroeconomic forecasts. *International Journal of Forecasting*, *4*, 363-376.

Boden, T. A., Marland, G., & Andres, R. J. (2017). Global, regional, and national fossil-fuel co2 emissions. *Carbon Dioxide Information Analysis Center, Oak Ridge National Laboratory, U.S. Department of Energy, Oak Ridge, Tenn., U.S.A.* doi: 10.3334/CDIAC/00001_V201

de Boyer Montgut, C., Madec, G., Fischer, A. S., Lazar, A., & Iudicone, D. (2004, 7). Mixed layer depth over the global ocean: An examination of profile data and a profile-based climatology. *J. Geophys. Res.*, *109*(C12003). doi: 10.1029/2004JC002378

Greene, W. H. (2003). *Econometric analysis (5th ed.)*. New Jersey: Prentice Hall.

Hamilton, E. J. (1994). *Time series analysis*. Princeton, New Jersey: Princeton University Press.

Hasselmann, K. (1976). Stochastic climate models, part i, theory. *Tellus*, *XXVIII*(6), 473-485.

Huang, Y., & Shahabadi, M. B. (2014). Why logarithmic? a note on thedependence of radiative forcing on gas concentration. *J. Geophys. Res. Atmos.*, *119*, 13,68313,689. doi: 10.1002/2014JD022466

Hubbert, M. K. (1962). *Energy resources*. National Academy of Sciences, Publication 1000-D.

Joos, F., Roth, R., Fuglestvedt, J. S., Peters, G. P., Enting, I. G., von Bloh, W., ... Weaver, A. J. (2013). Carbon dioxide and climate impulse response functions for the computation of greenhouse gas metrics: a multi-model analysis. *Atmospheric Chemistry and Physics*, *13*(5), 2793–2825. Retrieved from `https://acp.copernicus.org/articles/13/2793/2013/` doi: 10.5194/acp-13-2793-2013

Ljung, G. M., & Box, G. E. P. (1978). On a measure of a lack of fit in time series models. *Biometrika*, *65*, 297-303. doi: 10.1093/biomet/65.2.297

Mainshausen, M., Vogel, E., & A, N. a. K. L. (2017). Historical greenhouse gas concentrations for climate modelling (cmip6). *Geosci. Model Dev.*, *10*, 2057-2116.

Morice, C. P., Kennedy, J. J., Rayner, N. A., & Jones, P. D. (2012). Quantifying uncertainties in global and regional temperature change using an ensemble of observational estimates: The hadcrut4 online. *Journal of Geophysical Research*, *117*, D08101. Retrieved from `http://data.giss.nasa.gov/gistemp/tabledata_v3/GLB.Ts+dSST.txt` doi: 10.1029/2011JD017187

Nehring, R. (2009). Traversing the mountaintop: world fossil fuel production to 2050. *Philos Trans R Soc Lond B Biol Sci*, *364*, 3067-3079.

Nelson, C. R. (1972). The prediction performance of the f.r.b.-m.i.t.-penn model of the u.s. economy. *American Economic Review*, *62*, 902-917.

Nydal, R., & Lövseth, K. (1983). Tracing bomb 14c in the atmosphere, 1962-1980. *Journal of Geophysical Research*, *88*, 3621-42.

Reid, J. (2019). "the fluid catastrophe". Newcastle upon Tyne: Cambridge Scholars Publishing.

Wang, Q.-G., Yu, C., & Zhang, Y. (2013). Improved system identification with renormalization group. In *International conference on control and automation* (p. 878-883). Hangzhou, China: ICCA.

Zeebe, R. E. (2011, May). On the molecular diffusion coefficients of dissolved CO,HCO3-, and CO32- and their dependence on isotopic mass. *Geochimica et Cosmochimica Acta*, *75*(9), 2483-2498. doi: 10.1016/j.gca.2011.02.010
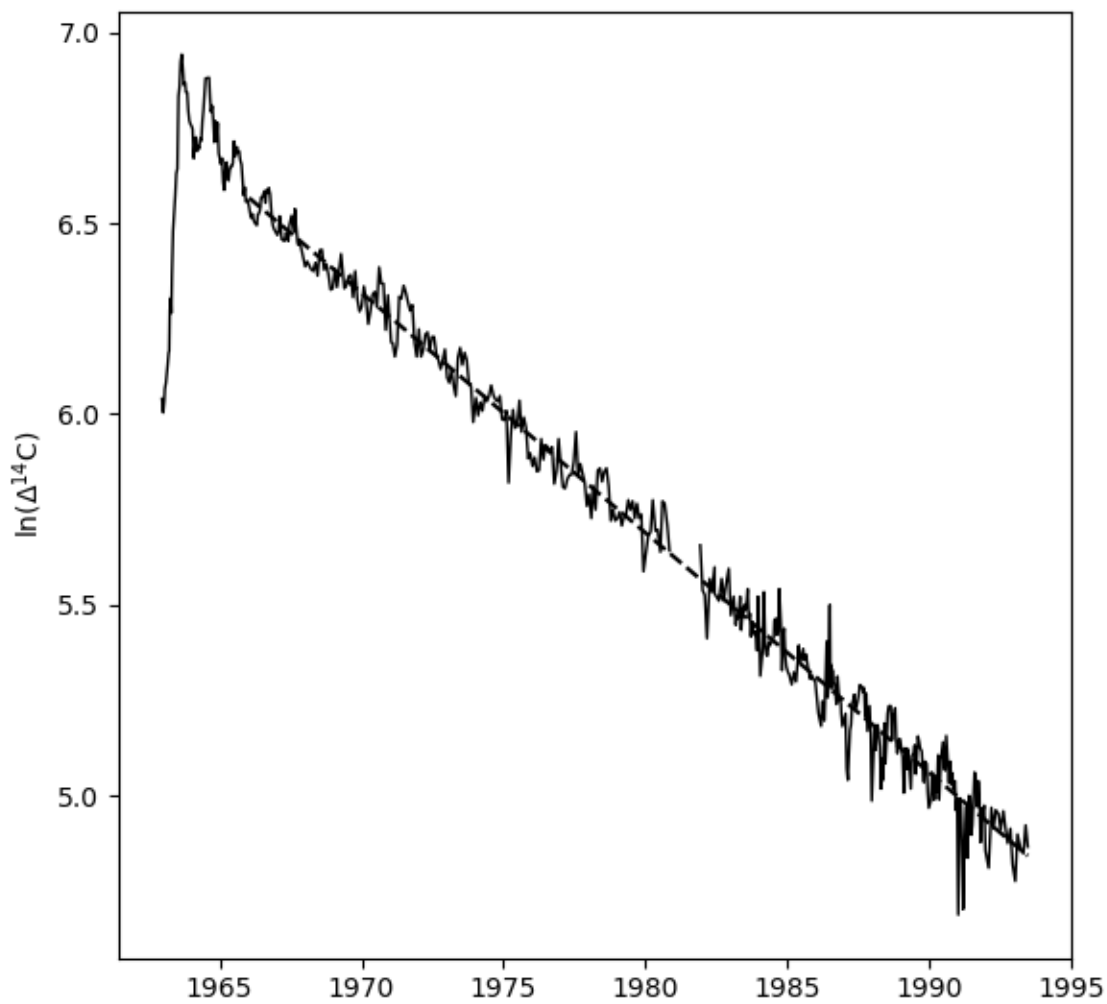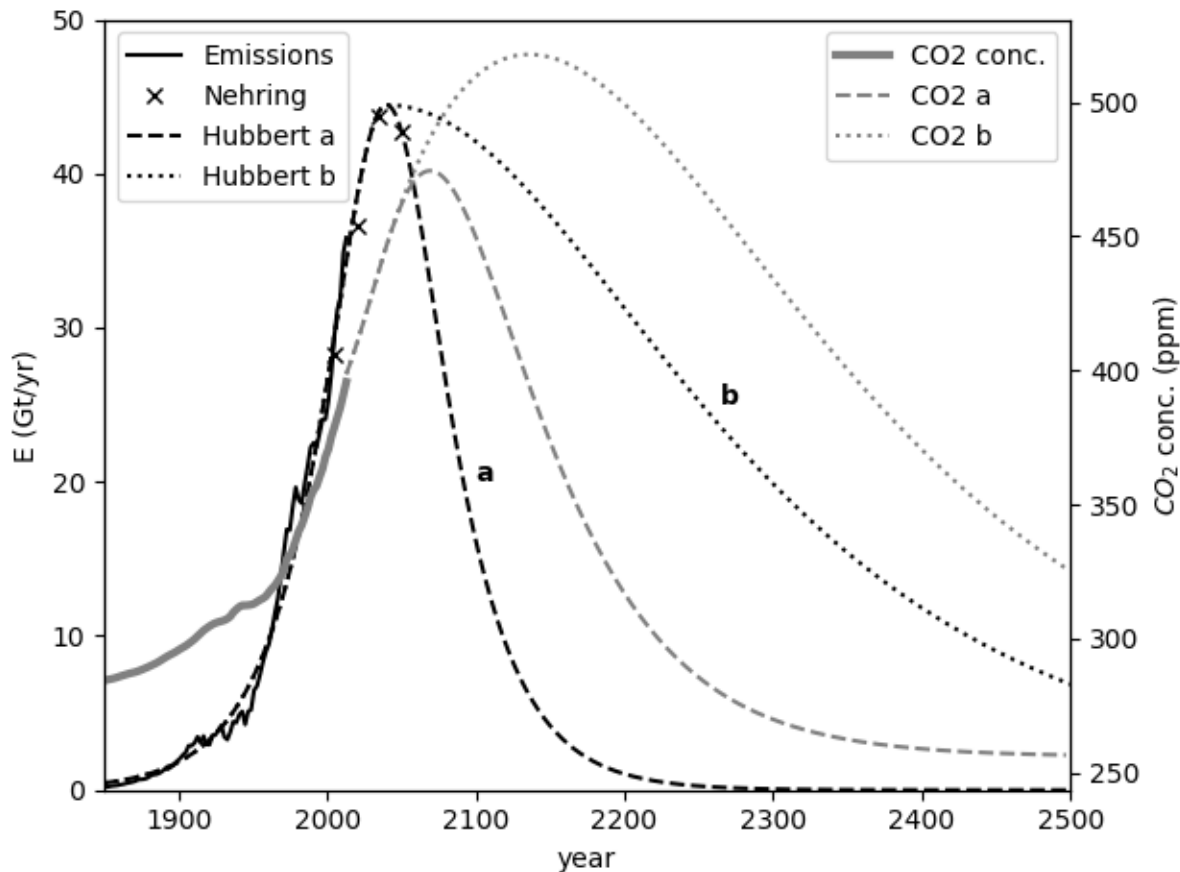
Figure 1.

Figure 2.

Figure 3.